

Complex Network Analysis of State Spaces for Random Boolean Networks

Amer Shreim,¹ Andrew Berdahl,¹ Vishal Sood,^{1,2} Peter Grassberger,^{1,2} and Maya Paczuski¹

¹*Complexity Science Group, Department of Physics and Astronomy,
University of Calgary, Calgary, Alberta, Canada, T2N 1N4*

²*Institute for Biocomplexity and Informatics, University of Calgary, Calgary, Alberta, Canada, T2N 1N4*

(Dated: June 21, 2024)

We apply complex network analysis to the state spaces of random Boolean networks (RBNs). An RBN contains N Boolean elements each with K inputs. A directed state space network (SSN) is constructed by linking each dynamical state, represented as a node, to its temporal successor. We study the heterogeneity of an SSN at both local and global scales, as well as sample-to-sample fluctuations within an ensemble of SSNs. We use in-degrees of nodes as a local topological measure, and the path diversity [1] of an SSN as a global topological measure. RBNs with $2 \leq K \leq 5$ exhibit non-trivial fluctuations at both local and global scales, while $K = 2$ exhibits the largest sample-to-sample, possibly non-self-averaging, fluctuations. We interpret the observed “multi scale” fluctuations in the SSNs as indicative of the criticality and complexity of $K = 2$ RBNs. “Garden of Eden” (GoE) states are nodes on an SSN that have in-degree zero. While in-degrees of non-GoE nodes for $K > 1$ SSNs can assume any integer value between 0 and 2^N , for $K = 1$ all the non-GoE nodes in an SSN have the same in-degree which is always a power of two.

PACS numbers: 05.45.-a, 89.75.-k, 89.75.Fb, 89.75.Da

I. INTRODUCTION

In this paper we apply complex network analysis to discrete, disordered, deterministic dynamical systems. The set of all trajectories of such a system can be described as a directed network. Each dynamical state is represented by a node and linked to its unique temporal successor by a directed link, giving the state space network (SSN). Thus the out-degree of a node is one. The irreversibility of the dynamics implies that a node can potentially have many in-coming links. The number of in-coming links at a node, or its in-degree, can vary from node to node, depending on the dynamical system considered. A wide dispersity of degrees characterizes many complex networks [2]. Therefore, complex network analysis may offer a useful alternative to traditional analyses of dynamical systems, such as the characterization of spatiotemporal patterns [3, 4, 5, 6, 7]. The first results of such an analysis on one dimensional cellular automata (CA) showed that heterogeneity of the SSNs at both the local and global scales distinguishes “complex” dynamics from simple dynamics [1]. Here we exploit complex network theory to characterize *disordered* dynamical systems by examining SSNs for ensembles of random Boolean networks.

Random Boolean networks (RBNs) were introduced by Kauffman [8] as models of gene regulation and have been extensively studied over the years by physicists as examples of strongly disordered systems [9, 10, 11, 12, 13]. The dynamics of each of the N Boolean elements in an RBN is given by a Boolean function of K randomly chosen input elements. Different realizations of the input elements and the Boolean functions for an RBN lead to an ensemble of RBNs for a given (N, K) .

In the thermodynamic ($N \rightarrow \infty$) limit RBNs exhibit a phase transition between chaotic and frozen phases passing through a critical phase for $K = 2$ [14]. In the frozen

phase, $K < 2$, the Hamming distance between two perturbations of the same state quickly die out. On the other hand, in the chaotic phase, $K > 2$, perturbations grow exponentially in time. Substantial analytical work has focused on the number of attractors as well as their lengths [15, 16, 17], which have been found exactly for $K = 1$ [18]. Krawitz and Shmulevich [19] computed the entropy of basin sizes and showed that for critical RBNs it scales with the system size. Otherwise, it asymptotes to a constant.

In unrelated developments, a variety of statistical methods have been established to characterize the structure of complex networks. Measures include probability distributions for the node degree, clustering (the tendency of nodes that share a common neighbor to also be linked to each other directly), motifs (overrepresented subgraphs in the network), etc. [2, 20, 21]. Many real world networks such as regulatory networks [22], the world-wide web [23], or the correlation structure of earthquakes [24, 25]) differ markedly from a random graph – where the degree distribution is Poisson and clustering is absent. They often display “fat-tailed” or even scale-free degree distributions.

In this paper we show that strong deviations from random graph behavior also occur in the SSNs of RBNs. In particular, for sufficiently small K , the probability distribution for the number of incoming links to nodes in the SSN, $P(k)$, has a fat-tail. In contrast, a randomly rewired null model for the SSN (*i.e.*, a random map) has Poissonian in-degree distributions. Also for small K , the maximum in-degree of any node in the SSN, k_{max} , displays scaling behavior with respect to size of the SSN, $\mathcal{N} = 2^N$. While k_{max} is a measure of local heterogeneity, we use the path diversity, \mathcal{D} , to characterize global heterogeneity [1]. We show that \mathcal{D} grows linearly with N for $K = 1$, while it grows faster than linearly with N for

$2 \leq K \leq 5$. For $K \geq 6$, \mathcal{D} scales with SSN size \mathcal{N} . In addition, for $K = 2$ (where RBNs are critical) the sample to sample fluctuations of \mathcal{D} are the largest and might be non-self-averaging [26, 27]. We speculate that SSN fluctuations at these three different scales (local, global, and sample to sample) for $K = 2$ RBNs are associated with criticality in the thermodynamic limit $\mathcal{N} \rightarrow \infty$.

A. Summary

In Section II we discuss the procedure used to construct RBNs, and their SSNs. The in-degree and the path diversity are also defined. In Section III A, we present results for the behavior of the nodes' in-degrees in an ensemble of SSN. In Section III A 2, we discuss the SSNs for $K = 1$ RBNs, which have unique features not shared by other K s. In Section III B, we examine the behavior of the path diversity. Discussion of our results and concluding remarks are found in Section IV.

II. DEFINITIONS

An RBN consists of N Boolean variables $\sigma_i = (0, 1)$ with $i = 1 \dots, N$. The dynamics of each element is determined by a Boolean function of K randomly chosen input elements,

$$\sigma_i(t+1) = f_i(\sigma_{i_1}(t), \sigma_{i_2}(t), \dots, \sigma_{i_K}(t)) \quad , \quad (1)$$

where $\sigma_{i_j}(t)$ is the value of the j^{th} input to σ_i at time t . The function f_i is randomly chosen to be 1 with probability p and 0 with probability $1-p$ for each set of values of its arguments. We consider only the case of unbiased RBNs with $p = 1/2$, except when $K = 1$. For that particular case, there are four possible boolean functions for each element. Instead of choosing them uniformly, using only the copy ($f(\sigma) = \sigma$) or the invert function ($f(\sigma) = \text{NOT}(\sigma)$) for each σ_i (with equal probability), leads to a critical $K = 1$ RBN [9].

We use synchronous update for the dynamics, *i.e.* all the Boolean elements in the network are updated in parallel at each time step. The networks are set up by choosing K different random inputs for each σ_i . While allowing self-connections, we do not allow multiple connections. We do not impose any connectivity constraint on the RBNs.

An RBN with N elements has $\mathcal{N} = 2^N$ different dynamical states. These states are nodes of a directed network. A link from **A** to **B** indicates that **A** evolves to **B** in one time step, making **B** the image of **A**, or **A** a pre-image of **B**. This directed network forms the state space network (SSN). The SSN typically consists of disconnected clusters, or basins of attraction. Each basin contains transient states, which are visited no more than once on any dynamical trajectory, and attractor states that may be visited infinitely often. Garden of Eden

states (GoE) are transient states that cannot be reached from any other state, *i.e.* they have no pre-images. Examples of some state space clusters are shown in Fig. 1 for $N = 9$ and different values of K .

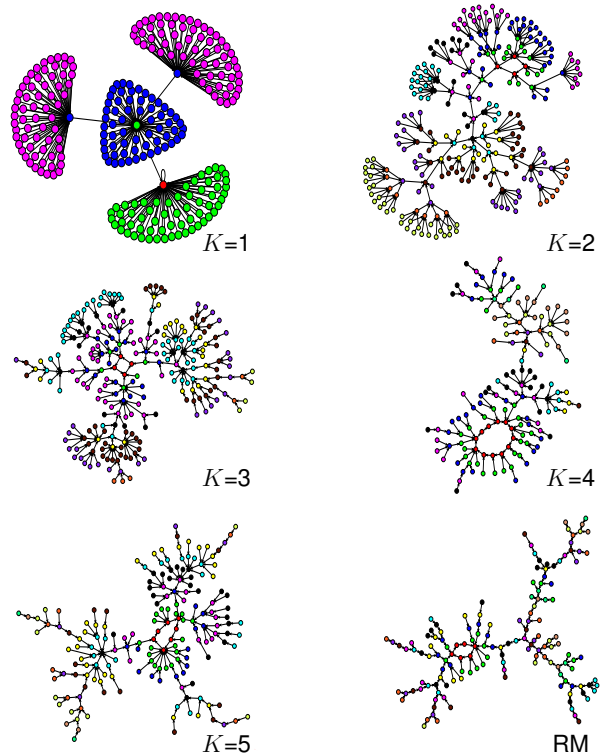


FIG. 1: (Color online). One connected cluster of an SSN for RBNs with $N = 9$ and different values of K displayed using the program 'Pajek' [28]. Nodes on the attractors are drawn in red; the other colors indicate distance from the attractor. Note that for $K = 1$ all nodes are either Garden of Eden states or hubs with all the hubs having the the same in-degree. RM stands for a random map.

Random maps are the limit of RBNs when $N, K \rightarrow \infty$ [29]. By construction, the state space of a random map forms an Erdős-Reyni random graph with a Poisson in-degree distribution, $P(k) = e^{-1}/k!$ with mean $\langle k \rangle = 1$. We constructed random map SSNs by picking the image of each node randomly from the $\mathcal{N} = 2^N$ possible nodes.

Identifying all attractors states and lumping them into a single node turns the SSN into a rooted tree. To study the global heterogeneity of this tree, we use path diversity \mathcal{D} . It quantifies topological variations in the paths connecting the GoE states to the root. It is similar to other global measures of tree like structures such as tree diversity [30] and topological depth [5]. \mathcal{D} measures the number of non-equivalent choices encountered when following each reversed path from the root to the GoE states.

Specifically, \mathcal{D} is computed as follows: each GoE state is assigned a diversity equal to one; a state with a single pre-image has the same diversity as its unique pre-image; and the diversity of a node with more than one incoming link is the sum of all *distinct* diversities of its pre-images

plus one. For instance, if a node has in-degree 6, and three of its pre-images have diversity 4, two have diversity 5, and the last has diversity 8, then that node's diversity is $4 + 5 + 8 + 1 = 18$. Finally, the path diversity \mathcal{D} of the entire SSN is the diversity of the root.

Table I provides a summary of the notation used. Note that we refer to nodes of the RBNs as “elements” and otherwise reserve the phrase “node” only for SSNs.

RBN	random Boolean network
N	number of elements of an RBN
K	number of inputs to each element of an RBN
SSN	state space network of an RBN
\mathcal{N}	number of nodes in an SSN ($\mathcal{N} = 2^N$)
k	in-degree of a node in an SSN
k_{max}	largest in-degree of a node in an SSN
\mathcal{D}	path diversity

TABLE I: Notations used in this paper.

III. RESULTS

A. In-Degree

1. Networks with $K \geq 2$

An elementary description of local heterogeneity of a network is its degree distribution. We computed in-degree distributions, $P(k)$, of the SSNs. These SSNs were obtained for RBNs with $1 \leq K \leq 10$ and $10 \leq N \leq 24$, as well as random maps of system sizes $10 \leq N \leq 24$. For $K = 1$ we distinguish between RBNs constructed using all four boolean functions and the critical $K = 1$ RBN discussed earlier. Fig. 2 presents $P(k)$ for SSNs with $N = 18$ ($\mathcal{N} = 2^{18}$). It is broad for $K = 1$, becomes narrower with increasing K , and converges for $K \rightarrow \infty$ to the in-degree distribution of the random map. The random map in-degree distribution itself converges to a Poissonian with $\langle k \rangle = 1$ when $N \rightarrow \infty$. Note that k for $K = 1$ only takes values 2^m . This is further discussed in Section III A 2.

The in-degree distribution $P(k)$ does not exhibit easily described behavior such as scaling. However, the results of Ref. [1] suggest that a more useful quantity is the largest in-degree k_{max} . Scaling behavior in k_{max} was shown to be a necessary but not sufficient signature of complex dynamics. Fig. 3a shows that

$$\langle \log_2 k_{max} \rangle \sim \nu_K N \text{ for } K \leq 6, \quad (2)$$

where the angular brackets indicate an average over different realizations of the RBN. The exponents ν_K appear to obey the relation:

$$\nu_K = -0.07(1)K + 0.68(1) \text{ for } 1 \leq K \leq 6. \quad (3)$$

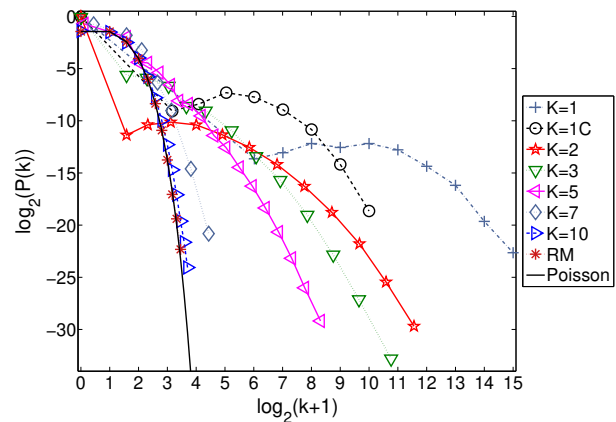


FIG. 2: (Color online). The in-degree distribution function, $P(k)$, for various connectivities, K , of the RBN, on a log-log scale. The distribution is computed for RBNs of size $N = 18$ by averaging the PDFs over 200 different realizations for each K . We used $k + 1$ instead of k on the x -axis, so that we could also show values for $k = 0$. The black solid line shows a Poissonian with $\langle k \rangle = 1$ for comparison.

For the system sizes studied, it is not possible to determine the asymptotic limit for larger K . However, the behavior for large K approaches the random map result.

For the random map, $P(k)$ tends to a Poissonian distribution when $N \rightarrow \infty$. If \mathcal{N} different values of k are chosen from a distribution $P(k)$, the expected maximum k_{max} can be related to \mathcal{N} by

$$\sum_{k=k_{max}}^{\infty} P(k) = \sum_{k=k_{max}}^{\infty} \frac{e^{-1}}{k!} = \frac{1}{\mathcal{N}}. \quad (4)$$

This gives the following exact bounds on k_{max} :

$$\frac{e^{-1}}{k_{max}!} \leq \frac{1}{\mathcal{N}} \leq \frac{e^{-1}}{k_{max}!} \sum_{m=0}^{\infty} \frac{1}{(k_{max})^m}.$$

Taking logarithms and using Stirling's approximation, the above equations yields for large \mathcal{N}

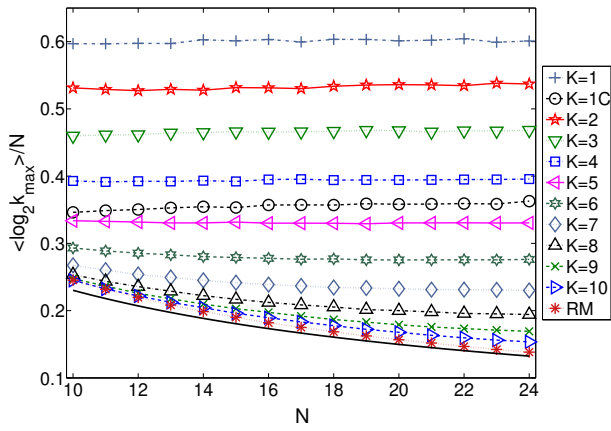
$$k_{max} \ln k_{max} \approx \ln \mathcal{N} = N \ln 2. \quad (5)$$

Finally we take logarithms again to get,

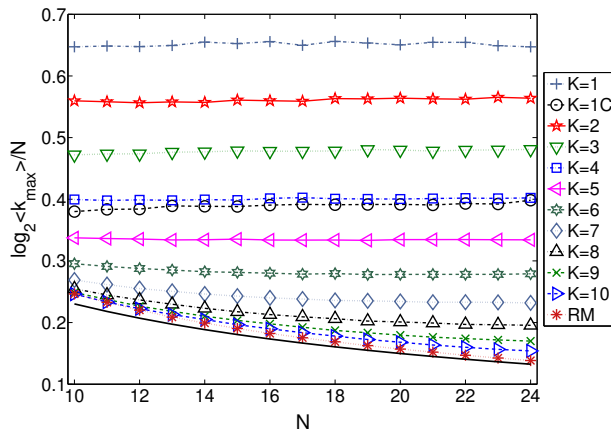
$$\log_2 k_{max} \approx \log_2 N. \quad (6)$$

As shown in from Fig. 3a, $\langle \log_2 k_{max} \rangle$ is very well described by Eq.(6) for random maps and RBNs with large K in the limit $N \rightarrow \infty$.

In order to see whether k_{max}/N is self averaging, *i.e.* whether the fluctuations of k_{max}/N become negligible for large N , we also plot in Fig. 3 the ratio $N^{-1} \log_2 \langle k_{max} \rangle$. A first look at Fig. 3 might suggest that both ways of averaging lead indeed to the same results, and self-averaging is satisfied. That this is not the case is demonstrated in Fig. 4, where we show the ratio



(a)



(b)

FIG. 3: (Color online). (a) The ratio $\frac{\langle \log_2 k_{max} \rangle}{N}$ is plotted against N . (b) The ratio $\frac{\log_2 \langle k_{max} \rangle}{N}$ is plotted against N . Both figures show systematic deviations from scaling for $K > 6$. The solid lines in (a) and (b) are $\frac{\log N}{N}$ and were plotted for comparison. The statistics, in this figure and Fig. 4 were obtained by sampling 2000 different realizations for each N and K .

$\langle \log_2 k_{max} \rangle / \log_2 \langle k_{max} \rangle$ versus N . We see from this figure that $\langle k_{max} \rangle$ scales with N as $\langle k_{max} \rangle \sim \mathcal{N}^{\tau_K}$ for $K \leq 6$, *i.e.* $\log_2 \langle k_{max} \rangle \sim \tau_K N$, similarly to Eq.(2). However, $\tau_K \neq \nu_K$. For large K it seems that that the fluctuations are less important, $\langle \log_2 k_{max} \rangle / \log_2 \langle k_{max} \rangle \rightarrow 1$ for $K \rightarrow \infty$.

The sample-to-sample fluctuations in k_{max} are captured by its probability distribution, shown in Fig. 5. We plot the probability distribution of $\log k_{max}$ multiplied by its standard deviation, $\sigma(\log_2 k_{max})$. The mean and standard deviation were computed independently for each N and K . The plots are well-fitted by a Gaussian for $2 \leq K \leq 6$, which suggests that $P(k_{max})$ is a log-normal, for sufficiently large N . For $K > 6$, the plots

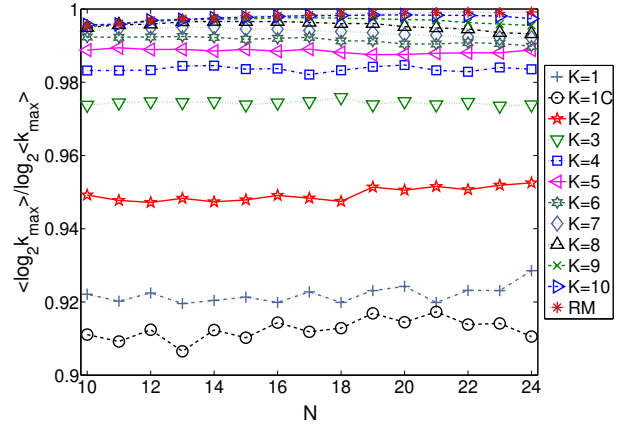


FIG. 4: (Color online). The ratio between the mean of the log and the log of the mean of the largest in-degree, $y \equiv \frac{\langle \log_2 k_{max} \rangle}{\log_2 \langle k_{max} \rangle}$, is plotted against the size of the RBN, N . If the two quantities were scaling with the same exponent, all curves should tend to $y = 1$ for large N . The plot shows that $\langle \log_2 k_{max} \rangle$ and $\log_2 \langle k_{max} \rangle$ are scaling with different exponents for $K \leq 6$.

indicate deviations from log-normal behavior.

2. $K=1$ Networks

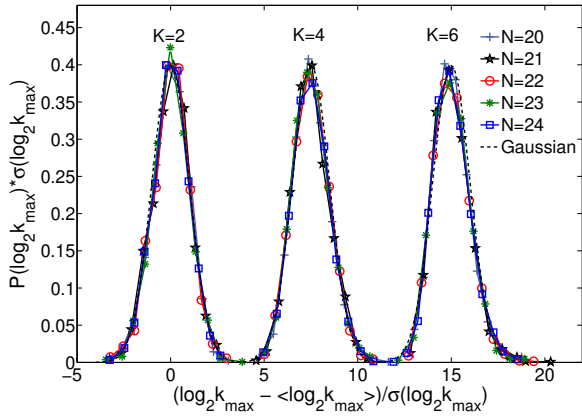
While $\log_2 k$ can take non integer values for $K \geq 2$, our simulations show that for $K = 1$, $\log_2 k$ takes only integer values. Accordingly, we fit $P(\log_2 k_{max})$ by a binomial instead of a Gaussian in Fig. 6. The parameters of the binomial, denoted here by n and s , were obtained by fitting them to the mean and the variance of the data,

$$\begin{aligned} \langle \log_2 k_{max} \rangle &= ns, \\ \sigma^2(\log_2 k_{max}) &= ns(1-s), \end{aligned} \quad (7)$$

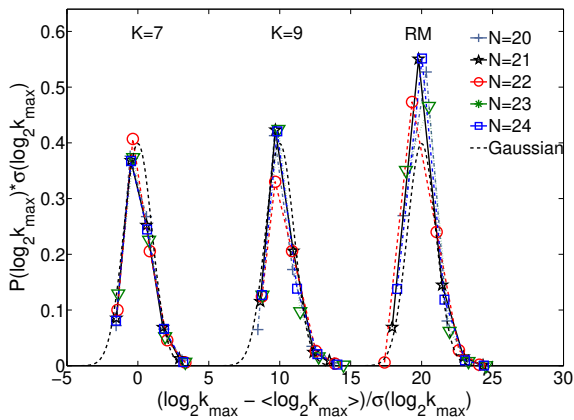
where the second line is the variance. Note that the above equation can give a non-integer value of n . The binomial distributions shown in Fig. 6 are constructed by rounding the best fit of n to its nearest integer value, while using the best fit values of s . Furthermore, we find that n linearly scales with N while s is independent,

$$\begin{aligned} n &= 0.79(1)N + 0.01(1), \\ s &= 0.75(1). \end{aligned} \quad (8)$$

For any $K = 1$ SSN, the in-degrees take only two different values: either $k = 0$ (for GoE states), or $k = 2^m$ with the same m for each non-GoE state on any given SSN. Since there are $\mathcal{N} = 2^N$ states, the number of non-GoE states is also a power of two and equals 2^{N-m} . We have checked that this is true in an ensemble of 10,000 randomly chosen RBNs with $10 \leq N \leq 24$ but we don't yet have a satisfactory analytical explanation for this result.



(a)



(b)

FIG. 5: (Color online). The rescaled PDFs of the log of the largest in-degree $P(\log_2 k_{max})$ for (a) $K = 2, 4$, and 6 , and (b) $K = 7, 9$, and the random map. The dashed lines are Gaussian distributions with mean zero and variance one. The plots indicate that k_{max} is distributed according to a log normal distribution for $K = 2, 4$ and 6 . Similar results hold for $K = 3$ and 5 . Deviations from the Gaussian distribution are seen for $K > 6$. In (a) the distributions for $K = 4$ and $K = 6$ were offset by 7.5 and 15 units on the x-axis for clarity of presentation. In (b) the distributions for $K = 9$ and the random map were offset by 10 and 20 units.

B. Path Diversity

Scaling of k_{max} with system size for $K \leq 6$, indicates asymptotic local heterogeneity of the SSNs. As shown in Ref. [1] local heterogeneity is often insufficient to distinguish simple from complex dynamics. A complimentary global topological measure, the path diversity, reveals simple behavior that many underly local heterogeneity. In Ref. [1] it was found that complex cellular automata show scaling behavior in both local and global measures. Here we investigate the path diversity of SSNs of RBNs.

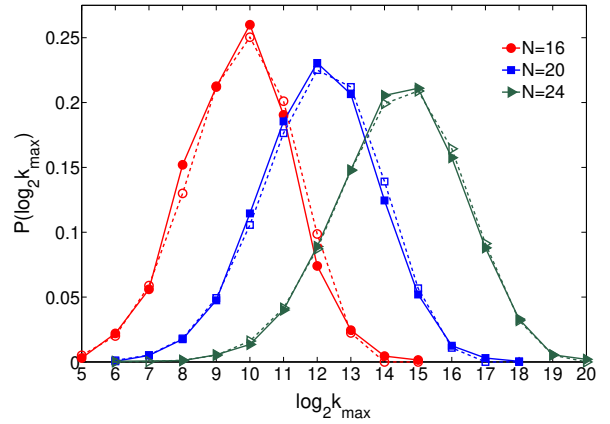


FIG. 6: (Color online). The PDF $P(\log_2 k_{max})$ of the log of the largest in-degree, $\log_2 k_{max}$ for $K = 1$ RBNs. The three dashed lines with empty symbols are binomial best fits given by Eq. 7.

Fig. 7 suggests that $\langle \log_2 \mathcal{D} \rangle \sim \zeta_K N$ for $K \geq 5$ and for the random map. However, the plots are not conclusive as to whether or not $\langle \log_2 \mathcal{D} \rangle$ becomes linear in N for $K < 5$, for large system sizes, or with large finite size corrections. Fig. 8 shows $\Delta_{\log_2 N} \langle \log_2 \mathcal{D} \rangle$, the discrete derivative of $\langle \log_2 \mathcal{D} \rangle$ with respect to $\log_2 N$. For $K = 1$, the figure indicates that $\langle \log_2 \mathcal{D} \rangle \sim \log_2 N$. A faster than logarithmic growth of $\langle \log_2 \mathcal{D} \rangle$ is seen for $K = 1$ critical and $K = 2$.

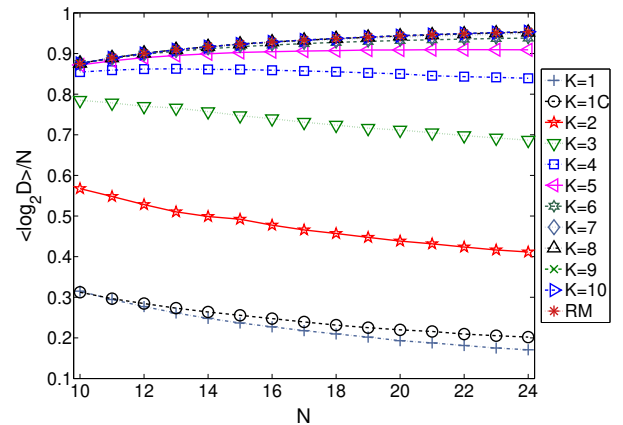


FIG. 7: (Color online). Log path diversity as a function of the system size. $\langle \log_2 \mathcal{D} \rangle / N$, is plotted as a function of N , for various values of K and the random map. For $K \geq 5$, $\langle \log_2 \mathcal{D} \rangle$ asymptotes to $\zeta_K N$, while the plots have the opposite curvatures for $K \leq 4$.

An example of a simple tree that exhibits logarithmic behavior of path diversity is the Cayley tree. On such an SSN each transient state has exactly z pre-images, except for the root which has $z+1$ pre-images. Given the symmetry of the Cayley tree, all the nodes at the same

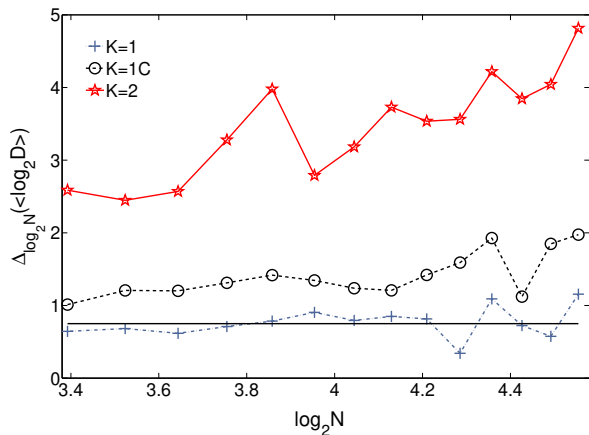


FIG. 8: (Color online). The discrete derivative of $\langle \log_2 \mathcal{D} \rangle$ with respect to $\log_2 N$, $\Delta_{\log_2 N} \langle \log_2 \mathcal{D} \rangle$, is plotted against $\log_2 N$ for $K = 1, 2$ and $K = 1$ critical. $\Delta_{\log_2 N} \langle \log_2 \mathcal{D} \rangle$ is defined as $\frac{\langle \log_2 \mathcal{D}_i \rangle - \langle \log_2 \mathcal{D}_{i-1} \rangle}{\log_2 N_i - \log_2 N_{i-1}}$. A horizontal line of this plot indicates a relationship of the form $\langle \log_2 \mathcal{D} \rangle \sim \log_2 N$. For the system sizes studied, the data suggests a logarithmic growth of $\langle \log_2 \mathcal{D} \rangle$ with respect to N . For $K = 1$ critical and $K = 2$, $\Delta_{\log_2 N} \langle \log_2 \mathcal{D} \rangle$ show growth trends which are indicative of a faster than logarithmic growth of $\langle \log_2 \mathcal{D} \rangle$ with N .

distance from the root will have the same path diversity. Furthermore, the path diversity is incremented by one with each step towards the root. This makes the path diversity equal to the depth of the tree which can be expressed in terms of the number of nodes \mathcal{N} :

$$\mathcal{D} = \log_z \{ (z-1)\mathcal{N} + 1 \}. \quad (9)$$

Thus the logarithmic growth of $\langle \log_2 \mathcal{D} \rangle$ for $K = 1$ networks suggests a different class of dynamical complexity than for $K \geq 2$ networks. Meanwhile, random map-like-scaling of $\langle \log_2 k_{max} \rangle$ for RBNs with sufficiently large K suggests relatively simple dynamics. However, on the basis of those two measures, one cannot cleanly distinguish the behavior of $K = 2$ critical RBN from that of $K > 2$ RBNs. We now show that sample-to-sample fluctuations in $\log_2 \mathcal{D}$ enable such a distinction.

We report the distribution of $\log_2 \mathcal{D}$, $P(\log_2 \mathcal{D})$, in Fig. 9. For a fixed system size, $P(\log_2 \mathcal{D})$ is broadest for $K = 2$ RBNs. To quantify the width of $P(\log_2 \mathcal{D})$, we study its variance. Fig. 10 shows that the variance of $\log_2 \mathcal{D}$, $\sigma^2(\log_2 \mathcal{D})$, grows fastest with N for $K = 2$. Unlike $\langle \log_2 k_{max} \rangle$ and $\langle \log_2 \mathcal{D} \rangle$, $\sigma^2(\log_2 \mathcal{D})$ shows non-monotonic behavior as a function of K . We interpret this as an indication that the criticality of $K = 2$ RBNs can be associated with large sample-to-sample fluctuations of its SSNs.

Generally, large sample-to-sample fluctuations in disordered media may lead to the absence of self-averaging. A canonical measure of self-averaging is the ratio:

$$\mathcal{R}(\mathcal{D}) = \frac{\langle \mathcal{D}^2 \rangle - \langle \mathcal{D} \rangle^2}{\langle \mathcal{D} \rangle^2}. \quad (10)$$

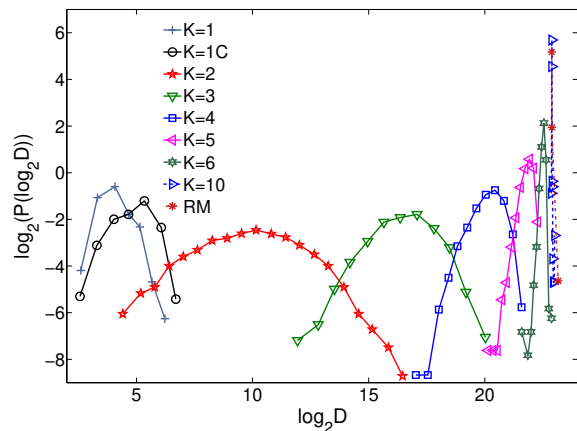


FIG. 9: (Color online). The log of the PDF of the log of the path diversity, $P(\log_2 \mathcal{D})$, for various values of K and $N = 24$. $P(\log_2 \mathcal{D})$ is the broadest for $K = 2$. $P(\log_2 \mathcal{D})$ becomes narrow for large values of K .

A system is said to be self-averaging with respect to \mathcal{D} if $\mathcal{R}(\mathcal{D})$ goes to zero for large N [26, 27]; otherwise, it is said to lack self-averaging. For the system sizes we are able to study, the evidence for or against self-averaging is not completely conclusive. Nevertheless, as indicated in the inset of Fig 10, $K = 2$ RBNs show the largest values for \mathcal{R} and are therefore the most likely to exhibit non-self-averaging behavior in the thermodynamic limit of large system size.

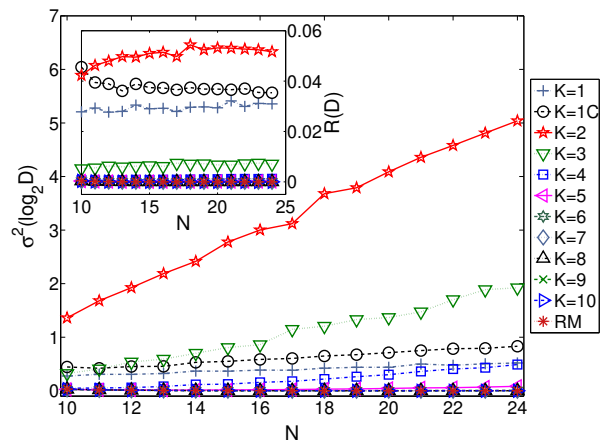


FIG. 10: (Color online). The variance of the log of the path diversity $\sigma^2(\log_2 \mathcal{D})$ is plotted as function of the size of the RBN, N , for various values of K . $\sigma^2(\log_2 \mathcal{D})$ shows non-monotonic behavior as a function of K , it grows the fastest for $K = 2$. On the other hand, $\sigma^2(\log_2 \mathcal{D})$ appears to tend to a constant or decreases with increasing N , for large values of K . For the random map, $\sigma^2(\log_2 \mathcal{D})$ is a decreasing function of N . The inset shows a plot of $\mathcal{R}(\mathcal{D}) = \frac{\sigma^2(\log_2 \mathcal{D})}{\langle \log_2 \mathcal{D} \rangle^2}$ as function of N . The data for $K = 2$ suggests that $\log_2 \mathcal{D}$ might be non-self-averaging in the thermodynamic limit.

IV. DISCUSSION AND CONCLUSION

We have studied the topology of state space networks (SSNs) for ensembles of random Boolean networks. Each dynamical state of the Boolean network corresponds to a node in the SSN and is linked to its successor state. We characterize the heterogeneity of these SSNs at the local, node, scale by the distribution of the in-degrees and the scaling of the largest in-degree. Global heterogeneity over all paths in the SSN is characterized by the path diversity. For elementary 1-d cellular automata, it was demonstrated in Ref. [1] that simultaneous scaling behavior in both k_{max} and \mathcal{D} indicates “complex” spatio-temporal dynamics (Wolfram class IV and partly class III). On the other hand, it was found in [1] that one or both of these does not scale for CA in class I or II – which all have simple dynamics.

As is well-known, RBNs exhibit a phase transition between chaotic ($K > 2$) and frozen ($K < 2$) behavior. $K = 2$ RBNs are critical and therefore more complex than RBNs with $K \neq 2$ which mainly show frozen ($K < 2$) or chaotic ($K > 2$) behavior [31]. In fact, RBNs in the frozen phase (e.g. $K = 1$) resemble class II CA as they almost always rapidly go to one of many attractors with a short period. In addition, RBNs in the chaotic phase resemble some class III CA in that they have long transients and attractors with large periods. We have investigated whether or not the different phases of RBNs can be distinguished on the basis of a topological analysis of the corresponding ensembles of SSNs, and the extent to which these phases overlap in the behavior of their SSNs.

We find that for $1 \leq K \leq 6$, $\log_2 k_{max}$ exhibits scaling as a function of the size of the SSN, $\langle \log_2 k_{max} \rangle \sim \nu_K N$. Recall N is the number of nodes in the Boolean network, and $\mathcal{N} = 2^N$ is the size of the SSN. The scaling exponent ν_K is largest for $K = 1$ and monotonically decreases for larger values of K . The $K, N \rightarrow \infty$ limit of the RBNs is the random map [29]. We have shown analytically that for the random map, $\log_2 k_{max} \sim \log_2 N$.

On the other hand, our numerical results indicate that $\langle \log_2 \mathcal{D} \rangle$ scales with the size of the SSN only for sufficiently large values of K ($K \geq 5$), $\langle \log_2 \mathcal{D} \rangle \sim \zeta_K N$. ζ_K is largest for the random map and monotonically decreases with decreasing K (which is the opposite of ν_K). For $K = 1$, $\langle \log_2 \mathcal{D} \rangle \sim \log_2 N$. For $2 \leq K \leq 5$, it is not clear from the data whether $\langle \log_2 \mathcal{D} \rangle$ scales linearly with N . It

is clear, however, that $\langle \log_2 \mathcal{D} \rangle$ grows faster-than-linear with $\log_2 N$.

Together, the absence of scaling for k_{max} and \mathcal{D} correctly rule out the random map (and most likely RBNs with large K) and $K = 1$ RBNs, from reporting high dynamical complexity. However, neither of these measures addresses sample-to-sample fluctuations, which are generally important in the characterization of disordered systems. We find that the probability distribution function of k_{max} converges to a log-normal distribution for $1 \leq K \leq 6$. While this is also seen for $\log_2 \mathcal{D}$, unlike the monotonic dependence of the variance of $\log_2 k_{max}$, the variance of $\log_2 \mathcal{D}$ does not vary monotonically with K . In fact, the variance grows the fastest with the size of the SSN for critical $K = 2$ RBNs. Numerical results also suggest that $\log_2 \mathcal{D}$ may possibly exhibit non-self-averaging behavior for $K = 2$.

Our results support the conclusion that heterogeneity in SSNs can be associated with complex dynamics in disordered systems. $K = 2$ RBNs are distinguished from other RBNs by simultaneously exhibiting three kinds of network heterogeneity. The first is a local heterogeneity on the node level indicated by the scaling of $\log_2 k_{max}$ with the size of the SSN. The second is a global heterogeneity on the trajectories level indicated by a faster-than-linear growth of $\log_2 \mathcal{D}$ with $\log_2 N$. Finally, there is a heterogeneity on the level of samples of RBNs, indicated by the fast growth of the $\sigma^2(\log_2 \mathcal{D})$ for RBNs with $K = 2$.

Additionally, we point out that many analytical results are known for $K = 1$ RBNs [16, 18] (and also for the random map, $K \rightarrow \infty$ [29]). In the present paper we found some striking numerical regularities for $K = 1$ which do not seem to follow directly from these. It will be interesting to see if some of the numerical results in this paper can be derived analytically. Here we list some of these results. 1) As discussed in Section III A 2, all non-GoE states in a $K = 1$ SSN have the same in-degree which is a power of two. This also makes the number of non-GoE states a power of two. 2) The distribution function of the largest in-degree of SSNs of $K = 1$ RBNs is consistent with a log-binomial distribution as shown in Fig. 6. 3) For $K = 1$ RBN, the path diversity scales with system size as $\langle \log_2 \mathcal{D} \rangle \sim \log_2 N$ as shown in Fig. 8. 4) The path diversity of the random map scales with the system size as $\langle \log_2 \mathcal{D} \rangle \sim \zeta_K N$, as shown in Fig. 7.

[1] A. Shreim, P. Grassberger, W. Nadler, B. Samuelsson, J. Socolar, and M. Paczuski, Phys. Rev. Lett. **98**, 198701 (2007).
 [2] M. E. J. Newman, SIAM Review **45**, 167 (2003).
 [3] S. Wolfram, *New Kind of Science* (Wolfram Media, 2002).
 [4] P. Grassberger, Int. J. Theor. Phys. **25**, 907 (1986).
 [5] R. Badii and A. Politi, Phys. Rev. Lett. **78**, 444 (1997).

[6] W. Bialek, I. Nemenman, and N. Tishby, Physica A **302**, 89 (2001).
 [7] D. P. Feldman and J. P. Crutchfield, Phys. Lett. A **238**, 244 (1998).
 [8] S. Kauffman, J. Theor. Biol. **22**, 437 (1969).
 [9] B. Drossel, *Random boolean networks* (2007), URL <http://www.citebase.org/abstract?id=oai:arXiv.org:0706.3351>
 [10] M. Aldana, S. Coppersmith, and L. Kadanoff,

In Perspectives and Problems in Nonlinear Science (Springer, New York, 2003), pp. 23–89.

- [11] B. Derrida and D. Stauffer, *Europhysics Letters* **2**, 739 (1986).
- [12] H. Flyvbjerg, *J. Phys. A: Math. Gen* **21**, L955 (1988).
- [13] U. Bastolla and G. Parisi, *J. Theor. Biol.* **187**, 117 (1997).
- [14] B. Derrida and Y. Pomeau, *Europhys. Lett.* **1**, 45 (1986).
- [15] B. Drossel, *Phys. Rev. E* **72**, 016110 (2005).
- [16] B. Drossel, T. Mihaljev, and F. Greil, *Phys. Rev. Lett.* **94**, 88701 (2005).
- [17] B. Samuelsson and C. Troein, *Phys. Rev. Lett.* **90**, 98701 (2003).
- [18] H. Flyvbjerg and N. Kjaer, *J. Phys. A: Math. Gen.* **21**, 1695 (1988).
- [19] P. Krawitz and I. Shmulevich, *Phys. Rev. Lett.* **98** (2007).
- [20] R. Albert and A. Barabasi, *Rev. Mod. Phys.* **74**, 47 (2002).
- [21] R. Milo, S. Shen-Orr, S. Itzkovitz, N. Kashtan, D. Chklovskii, and U. Alon, *Science* **298**, 824 (2002).
- [22] R. Albert, *J. Cell Science* **118**, 4947 (2005).
- [23] A. Barabasi, R. Albert, and H. Jeong, *Physica A* **281**, 69 (2000).
- [24] M. Baiesi and M. Paczuski, *Phys. Rev. E* **69**, 066106 (2004).
- [25] J. Davidsen, P. Grassberger, and M. Paczuski, *Geophys. Res. Lett.* **33**, L11304 (2006).
- [26] H. Chamati, E. Korutcheva, and N. Tonchev, *Phys. Rev. E* **65**, 26129 (2002).
- [27] S. Wiseman and E. Domany, *Phys. Rev. Lett.* **81**, 22 (1998).
- [28] <http://vlado.fmf.uni-lj.si/pub/networks/pajek/>.
- [29] B. Derrida and H. Flyvbjerg, *J. Physique* **48**, 971 (1987).
- [30] B. A. Huberman and T. Hogg, *Physica D* **2**, 376 (1986).
- [31] S. Kauffman, *The Origins of Order* (Oxford Univ. Press, 1993).